

Skinning a robot: Design Methodologies for Large-Scale Robot Skin

Thuy-Hong-Loan Le

École de Technologie Supérieure
Montreal, Quebec, Canada

Email: thuy-hong-loan.le.1@ens.etsmtl.ca

Perla Maiolino

Department of Computing, Goldsmiths
University of London, U.K.

Email: p.maiolino@gold.ac.uk

Fulvio Mastrogiovanni, Giorgio Cannata

University of Genoa
Genoa, Italy

Email: f.mastrogiovanni@unige.it

Abstract—Providing a robot with large-scale tactile sensing capabilities requires the use of design tools bridging the gap between user requirements and technical solutions. Given a set of functional requirements (e.g., minimum spatial sensitivity or minimum detectable force), two prerequisites must be considered: (i) the capability of the chosen tactile technology to satisfy these requirements from a technical standpoint; (ii) the ability of the customisation process to find a trade-off among different design parameters, such as (in case of robot skins based on the capacitive principle) dielectric thickness, diameter of sensing points, or weight. The contribution of this paper is two-fold: (i) the description of the possibilities offered by a design toolbox for large-scale robot skin based on Finite Element Analysis and optimisation principles, which provides a designer with insights and alternative choices to obtain a given tactile performance according to the scenario at hand; (ii) a discussion about the intrinsic limitations in simulating robot skin.

I. INTRODUCTION

Robots operating in dynamic and unstructured environments must exhibit advanced forms of interaction with objects and humans. Such concepts as *shared workspace* and *robot co-worker* require novel solutions in human-robot interaction processes. Large-scale tactile sensing can play a fundamental role in enhancing perceptual, cognitive and operative capabilities of robots, specifically when they physically interact with objects and humans in the environment.

In the past three decades, many solutions to design, engineer and manufacture tactile sensors have been presented and discussed in the literature [1]. Tactile sensors based on the capacitive principle have been widely adopted in Robotics given their small size and the availability of low-cost readout electronics [2]. This allows designers and engineers not only to develop *ad hoc* solutions (e.g., robot fingertips), but also to obtain sensor arrays with hundreds or thousands tactile elements, which are able to cover wide areas of a robot body, such as robot hands, arms and torsos [3].

The concept of *large-scale* tactile sensing gives rise to a number of system-level challenges, which simply do not show up when focusing on small tactile sensor arrays. On the one hand, robot skin aimed at covering the whole surface of humanoid robots (which approximately amounts to 2 m^2 in accordance with the typical surface of human bodies) must be modular, conformable, easy to manufacture [3] and deploy [4]. Since the majority of the current humanoid robot platforms are not endowed with robot skin natively, the need arises to take

into account such issues as infrastructure and networking (with specific emphasis on the internal cabling) [5], calibration (both taxel spatial locations and responses must be considered) [6], fault-tolerance (given safety issues related to the fact that the robot may purposively be in contact with objects and humans) and distributed processing (given tight real-time requirements originating from such a *distributed* sensor) [7].

In this perspective, two trends in robot skin design and fabrication can be observed nowadays: the first is related to the use of *standard* (i.e., easy to manufacture with common equipment and limited cost) electronics as a substrate, such as conformable Printed Circuit Boards (PCBs); the second employs novel forms of flexible and stretchable substrates [8], also including commercial prototypes, such as Stretch-Sense^{TM1}, and even textiles. As a matter of fact, the first class includes modular and scalable robot skin prototypes, which can be applied to large surfaces of a robot body, but typically is neither stretchable nor can be conformed when curvatures are too high. Approaches belonging to the second class aim at overcoming these limitations, but it is not common yet to read in the literature about scalable and modular solutions.

The design process of robot skin involves a trade-off between user requirements and geometrical as well as physical parameters. Robot engineers need tools to design solutions meeting such functional requirements as, e.g., minimum detectable force, spatial and temporal sensor resolution, or overall weight. These requirements impact on sensing capabilities (e.g., to detect gentle touches or to manipulate objects), as well as on system-level design, including the embedded networking architecture and tactile data processing algorithms.

In this paper, we present a robot skin design toolbox² developed to aid robot designers and engineers in the process of creating custom versions of robot skin. The toolbox allows them to: (i) analyse the sensor's behaviour considering both single transducers and large-scale configurations, which imply issues related to generic robot surfaces, such as the definition of geometric parameters (e.g., size and pitch of tactile elements), elastomer thickness, as well as physical properties like the elastic modulus, the Poisson's ratio and the dielectric permittivity, or the overall robot skin weight; (ii)

¹Please refer to: <http://stretchsense.com/>.

²The toolbox is released as open source software. Check the current version at: <https://github.com/macilab/skin-toolbox>.

determine the most appropriate selection of parameter values, which constitute a good trade-off among design choices and functional requirements.

Although the toolbox has been designed with a specific robot skin technology in mind, namely ROBOSKIN [3], [2], specifically focused on large-area tactile sensing and belonging to the first class of approaches outlined above, in principle it can be adapted to model the behaviour of other capacitance-based robot skin designs (provided that a multiphysics model is available and it can be parameterised), being in large part agnostic with respect to the actual employed technology. The toolbox integrates Finite Element Methods (FEM), used to model the physics of the considered sensors, and optimisation approaches, used to define an appropriate trade-off between parameters and user requirements.

Classical approaches based on Contact Mechanics and FEM have been used to simulate and analyse the behaviour of material surfaces [9], including those embedding tactile sensors [10]. FEM analyses assuming different transduction principles have been reported (see the work described in [11], [12], [13] and the references therein). FEM-based approaches are typically preferred over other methods because: first, they allow for modelling tactile sensors in a realistic way, insofar they capture sensor geometry and boundary conditions more faithfully than other techniques [14]; second, FEM-based tools are commercially available and can serve for benchmarking and validation purposes.

Unfortunately, the approaches aimed at analysing the behaviour of robot skin are just a few. The aforementioned approaches are focused on single transducers, and do not consider the analysis of large-scale tactile surfaces nor the effect of varying parameter values. It has been only with the work described in [15] that the role of different design parameters (e.g., elastomer's thickness or shore, spatial resolution) have been considered, but only to a limited extent.

The availability of a design toolbox for robot skins is expected to greatly accelerate the adoption of such a technology for practical robot applications.

II. REFERENCE TECHNOLOGY AND MANUFACTURING ASPECTS

A. The Reference Robot Skin Technology

The robot skin technology we target in this work, called ROBOSKIN, has been described in [3]. As it is common for modular capacitance-based sensors, a single transducer (i.e., a tactile element, referred to as a *taxel*) is made up of three layers: the lower layer is a positive electrode, mounted on a conformable PCB; the upper layer is a ground electrode; the central layer is a soft elastomer serving as a dielectric between the two electrodes [10].

In ROBOSKIN, taxels are arranged in triangular modules, and different modules can be configured in *patches* to cover larger areas (Figure 1). Each module hosts 12 taxels, and (on the other side) the readout electronics, i.e., a small Capacitance to Digital Converter (CDC) chip (AD7147 from Analog

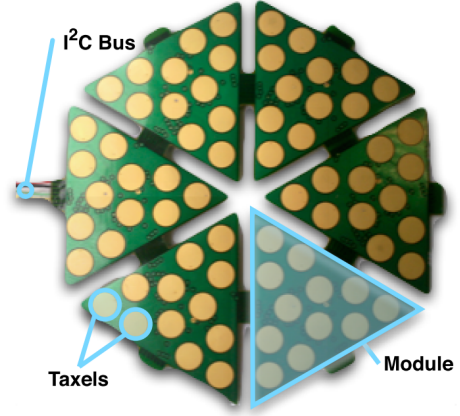


Fig. 1. The reference robot skin: a hexagonal patch divided into six triangular modules.

Devices). The CDC chip measures variations in capacitance values within a $4 - 30 \text{ pF}$ range with a sensitivity of 0.32 fF .

Normal forces exerted on the tactile surface produce variations in capacitance values reflecting the varied pressure on taxels. Ideally, the capacitance C associated with each taxel linearly depends on the dielectric constant ϵ_0 , the relative static permittivity of the dielectric material ϵ_r , the overlap area A and the distance d (i.e., the thickness of the dielectric) between the two electrodes:

$$C = \epsilon_0 \epsilon_r \frac{A}{d}. \quad (1)$$

Considering (1), the CDC output value for each taxel corresponds to:

$$\Delta C = C_p - C_n = \epsilon_0 \epsilon_r A \frac{d_n - d_p}{d_p d_n}, \quad (2)$$

where C_p and d_p are, respectively, the capacitance value and the elastomer thickness in the *contact* case (i.e., when a pressure is exerted), whereas C_n and d_n correspond to the *no contact* or nominal case. A pressure exerted on taxels produces a capacitance increase, i.e., $\Delta C > 0$ corresponds to a contact situation.

B. Manufacturing Aspects and Toolbox Use

The ROBOSKIN structure depends on the considered robot part (e.g., torso *versus* fingertips), required sensitivity, and function. ROBOSKIN has been used in three well-known humanoid robots [3], in a Schunk manipulator and in an industrial gripper used for clothes manipulation [16].

The design toolbox is used throughout the robot skin manufacturing process. In particular:

- (a) Definition of the patches covering *at best* a robot body part, Figure 2(a), and identification of the modules wiring pattern [4]. The analysis module verifies user requirements in terms of (both mechanical and electrostatic) contact properties.

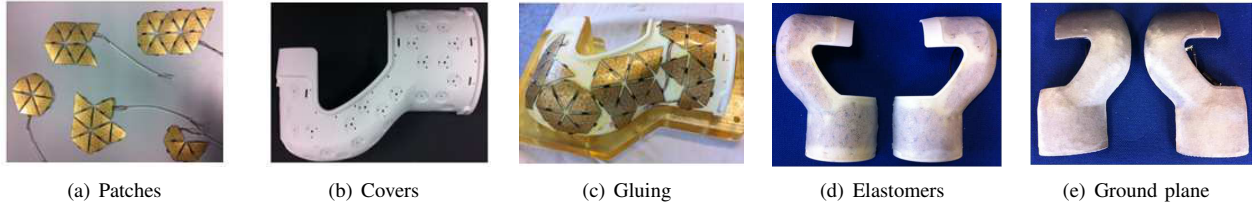


Fig. 2. Production steps for covering a link of a Schunk LW7 manipulator.

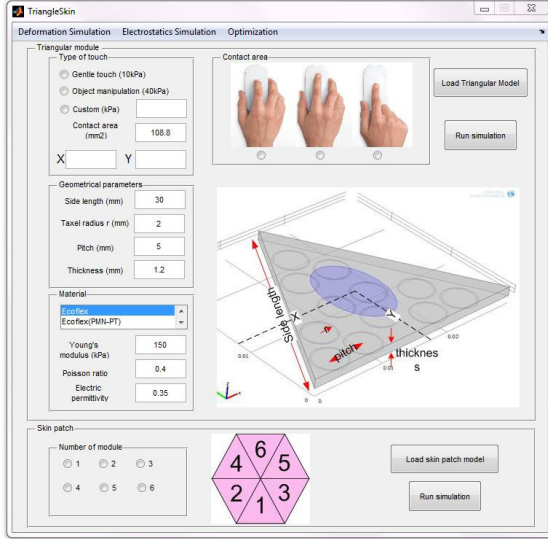


Fig. 3. The main interface of the robot skin design toolbox.

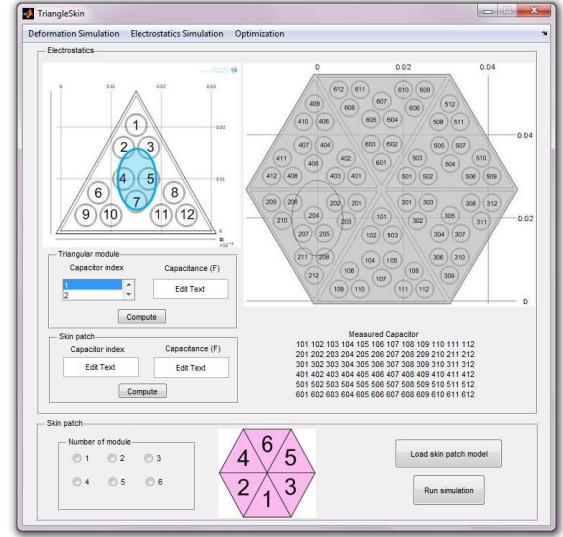


Fig. 4. The interface of the analysis component.

- (b) Manufacturing of the cover hosting robot skin patches, Figure 2(b). Round holes allow for embedding CDC chips and other ancillary electronics.
- (c) Bonding of the PCBs on the cover, Figure 2(c). In this phase, the conformability of the PCB and the triangular shape allow for a good robot skin bending performance up to a minimum curvature radius of about 1 cm.
- (d) Covering of the PCBs with the selected elastomer, Figure 2(d). The toolbox proposes alternative materials to use, on the basis of their physical characteristics (see Section III-B). The optimisation module suggests suitable elastomers according to user requirements related to sensitivity and density.
- (e) Covering of the elastomer with an appropriate ground plane, to allow for detecting contact with non-conductive objects, Figure 2(e).

III. THE TOOLBOX ARCHITECTURE

The design toolbox has been developed using COTS and custom software. The core of the architecture is the interface between COMSOL Multiphysics and MATLAB³. COMSOL Multiphysics allows for the creation of a multiphysics model of the patch of interest and the simulation of contact phenomena

using FEM analyses. The multiphysics analysis considers both *structural mechanics* and *electrostatics*, since induced mechanical deformations influence electrical responses and therefore sensory data. The structural mechanics component allows for the computation of deformations, forces, stresses and strains within the modelled patch. As a result of the pressure applied to the elastomer, strains and displacements are computed. A deformed mesh is produced, which is fed to the electrostatics component. An electric potential is applied between taxels and the ground plane located above the elastomer. This induces a set of capacitance variations proportional to their plates charge. Since, at a given time instant, the deformed mesh is fixed, electric phenomena can be studied under electrostatic conditions. MATLAB has been adopted to provide users with a friendly and intuitive user interface, which is fundamental in real-world use cases, Figure 3. Through the MATLAB interface, users can customise the COMSOL simulation and analyse results. Furthermore, it provides a bridge to the toolbox's optimisation component developed in MATLAB (described in Section III-B).

The toolbox is made up of two components:

- The *analysis* component (Section III-A) allows for FEM analyses and simulation of tactile sensors at different levels of detail. It is possible to set geometrical and

³Please refer to: www.comsol.com and www.mathworks.com.

mechanical parameters, as well as application-related parameters, and analyse the sensor's performance under those operating conditions.

- The *optimisation* component (Section III-B) specifies application-related requirements in terms of involved contact forces. It provides insights for selecting the elastomer maximising sensitivity in the chosen force range, minimising the overall robot skin weight, or both.

A. The Analysis Component

For robot skin design and customisation, available models based on capacitive transducers are parameterised with respect to patch's geometry, elastomer's properties and the characteristics of contact phenomena (Figure 3 on the left).

Geometric properties. The geometry of the basic RO-BOSKIN triangular module is parameterised in many aspects:

- The *taxel's radius* affects the size of the smallest detectable contact area. *Default: 2 mm.*
- The *taxel's pitch* is the distance between nearby taxels: a higher pitch is associated with a lower spatial resolution. *Default: 5 mm.*
- The *module's side* can be chosen by a designer according to specifications related to spatial resolution, which depend on the body part the module must be fixed to. If a lower spatial resolution is allowed, the module size can be increased. *Default: 30 mm.*
- The *elastomer's thickness* has a great impact on capacitance values, since it corresponds to the distance parameter d in (1). *Default: 2 mm.*

Dielectric properties and Rheological Characterisation. The elastomer's electrical and mechanical characteristics are essential to the sensor behaviour [15]. Different elastomers have been characterised both from the mechanical (in the static strain variation range between 5 – 30%, dynamic strain equal to 2% and at a 10 Hz frequency) and electrical response perspectives (at a frequency between 10 – 10⁸ Hz) and included in the toolbox database. A comprehensive analysis about such a characterisation has been reported in [10]. Both *bulk* elastomers (e.g., Polytek Polyurethane, Smooth-on Ecoflex 00 – 30) and *compounds* made up of base rubbers (e.g., SomaFoama, Polytek, Ecoflex 00 – 30) with 50% wt. of different ceramic fillers (e.g., Dioxide Titanate, TiO₂, Strontium Titanate, SrTiO₃ and lead magnesium niobate-lead titanate, PMN-PT) have been considered. Table I and Table II report experimental values for dielectric permittivity and the Young Modulus, respectively, in two relevant pressure ranges (as explained below) for all the compounds.

The toolbox allows for choosing among the available elastomers and simulating the sensor behaviour accordingly. This feature is particularly desirable since material characterisation procedures are usually expensive and time-consuming. It is noteworthy that, since the available equipment allowed us to characterise elastomers only in the 5 ÷ 30% range for static strain, the corresponding characterised stress ranges between 0 ÷ 55 kPa, with the maximum value depending on each elastomer. In order to give toolbox users the opportunity to

TABLE I
DIELECTRIC PERMITTIVITY OF THE ELASTOMERS AT 250 kHz.

	Pure	+ TiO ₂	+ SrTiO ₃	+ PMN-PT
Elastomer	ϵ_r	ϵ_r	ϵ_r	ϵ_r
SomaFoama	2.3	3.9	4.8	3.1
Ecoflex	4.2	-	5.2	5.3
Polytek	8.2	-	-	-

TABLE II
YOUNG MODULUS OF THE TESTED ELASTOMERS [MPa] FOR A COMPRESSIVE STRESS IN TWO RELEVANT PRESSURE RANGES: *gentle touch* (GT, 0 – 10 kPa) AND *manipulation-like touch* (MT, 10 – 100 kPa).

		Pure	+ TiO ₂	+ SrTiO ₃	+ PMN-PT
Elastomer	Range	E'	E'	E'	E'
SomaFoama	GT	0.13	0.36	0.39	0.16
	MT	0.13	0.49	0.45	0.21
Ecoflex	GT	0.18	-	0.33	0.25
	MT	0.20	-	0.49	0.32
Polytek	GT	0.19	-	-	-
	MT	0.46	-	-	-

simulate higher pressure values, we performed a third-order spline interpolation of the characterised curve for pressure ranges outside the characterised range until 100 kPa. Furthermore, it is possible to specify the most relevant material's parameters. Among them:

- The *Young modulus*, defined as $E = \sigma/\epsilon$, where σ and ϵ are the material's stress and strain, respectively [17]. The Young modulus is used to compute the elastomer's strain under an exerted pressure.
- The *Poisson's ratio* is a measure of the Poisson effect originating from the elastomer expansion along the direction normal to pressure application.
- The *dielectric permittivity* impacts on capacitance variations. For technological reasons, there is a lower bound to the transducer's detectable capacitance variation, in our case it is 0.32 fF. According to (1), the lower bound is a constraint relating taxel's area A , elastomer's thickness d and dielectric permittivity ϵ_r . In order to obtain the same sensitivity, an increased dielectric permittivity allows for a decreased taxel's area (therefore increasing robot skin sensitivity to small indentation) or for an increased elastomer's thickness (therefore increasing safety and allowing for high pressures contact).

Selecting the most appropriate material for simulation is important. The default material is Smooth-on SomaFoama, which is also used in the experiments reported in Section IV. It is characterised by many advantages, namely high compliance, easy handling during manufacturing and low weight. Since the material originates from a fast chemical reaction, the presence of air bubbles may determine a significant density variability, which may cause a differing mechanical behaviour between any two samples. Figure 5(a) shows the average and the standard deviation of the tactile sensor's response (using

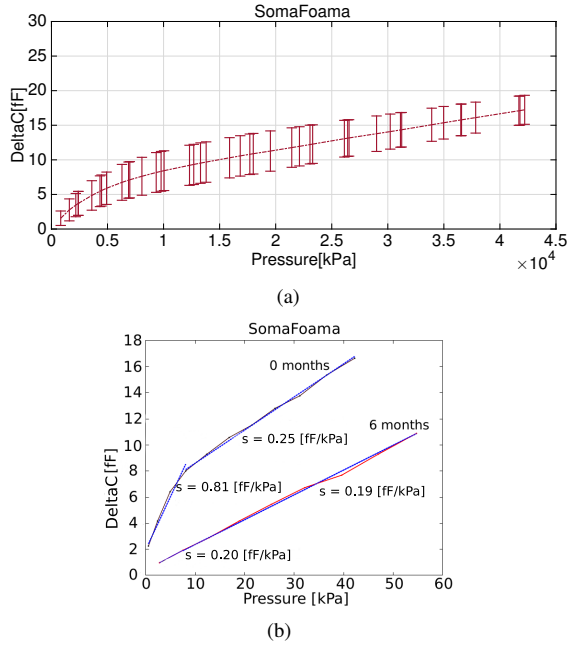


Fig. 5. (a) Average and standard deviation of the sensor response for different specimens of SomaFoama. (b) The sensor response for SomaFoama for a newly made sample (0 months) and for the same sample measured after a 6-month ageing process: *dotted lines* represent the linear interpolation of the data in the two ranges; s represents the sensitivity value expressed as the angular coefficients of the interpolating lines.

different specimens of SomaFoama) as a consequence of different pressure values. The maximum variation corresponds to 33% in the sensor response range. A variability in the mechanical characteristics between different samples of the same material is common to all the elastomers. Furthermore, ageing significantly alters the mechanical properties of elastomers leading to a change in the stress-strain curve. An extensive analysis of these aspects has been reported in [10]. Figure 5(b) shows the response of the sensor using a new sample of SomaFoama as a dielectric layer, and the response obtained after 6 months. We observe that the sensor's sensitivity decreases in all the pressure range, but more in the lower range. Furthermore, an overall *flattening* of the response is visible, which is likely due to an increase of the material stiffness. Such a variability poses interesting challenges for a faithful simulation: on the one hand, simulation is based on a *particular and specific* elastomer sample, which has been subject to a peculiar characterisation and that requires a new characterisation after some time due to the ageing issue; on the other hand, robot skin patches with other samples of the same type of elastomer may exhibit a slightly different behaviour.

Contact modeling. Robot skin designers must have an estimate of how contacts are detected in terms of pressure and contact areas. The toolbox provides insights for typical contact tasks. A literature survey shows that two broad classes of contacts can be identified on the basis of pressure ranges [18]. The first class is referred to as *gentle touch* and is characterised by contact pressures in the 0 – 10 KPa range,

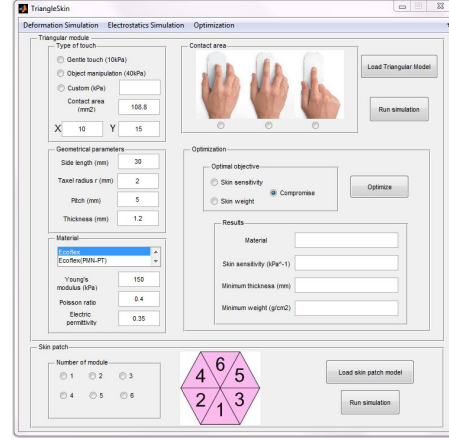


Fig. 6. The interface of the optimisation component.

whereas the second class, namely *manipulation-like touch*, involves pressures in the 10 – 100 KPa range. Users can also provide a custom distribution of pressure values.

Simulation of complex contact phenomena is an active research topic [19], [20]. Beside theoretical considerations about the nature of contact models [9], major problems arise at the computational level. Although these issues are outside the scope of this paper, we tried to find a trade-off between realistic contact scenarios and manageable simulations, which are *simple enough* to be computationally tractable. We focused on contact areas as much similar to human fingertips as possible, since contact modelling in grasping and manipulation tasks represents a significant part of the research activities in the field [1]. To this aim, we performed simple experiments to obtain information about fingertip contact areas. We asked 12 subjects to perform everyday common touch tasks, such as operating the touch screen of a mobile phone, typing on a keyboard and clicking mouse buttons. Each experiment has been performed by each subject 4 times, in order to obtain a statistically significant number of trials. For each trial, the *average shape* of the contact area and the exerted pressure are recorded and used in the toolbox. All these contact areas can be actually used in simulations.

B. The Optimisation Component

The optimisation component guides a user with the selection of the proper elastomer (Figure 6). Given a target contact pressure p_t (possibly labelled as gentle or manipulation-like touch), elastomers available in the database are evaluated based on two criteria, i.e., overall sensitivity and weight. A high sensitivity corresponds to a high variation in the sensor response, in our case a variation of the measured capacitance, with respect to a small variation in the applied pressure. The overall robot skin weight is an important parameter to consider,

specifically when large areas of a robot body must be covered, since it has a non negligible impact on control (impacting on maximum payload and maximum exerted torque). We employ two optimisation approaches:

- *Single-objective optimisation* maximises the robot skin sensitivity or minimises its overall weight, respectively, for the selected target pressure.
- *Multi-objective optimisation* selects the elastomers which are a trade-off between sensitivity and weight.

Sensitivity optimisation. In our case, sensitivity S is defined as the ratio between the variation of capacitance ΔC and the variation of the exerted pressure ΔP (i.e., the stress) in the *contact* and *no contact* cases, normalised with respect to C_n , introduced in (2):

$$S = \frac{1}{C_n} \frac{\Delta C}{\Delta P}. \quad (3)$$

Referring to $d_p - d_n$ as the variation of the elastomer thickness, and applying (1), an absolute measure of the sensitivity is expressed as:

$$S = \frac{1}{\varepsilon_0 \varepsilon_r \frac{A}{d_n}} \frac{\varepsilon_0 \varepsilon_r A (d_n - d_p)}{\Delta P d_n d_p}. \quad (4)$$

If we substitute the strain $\varepsilon = \Delta d/d_n$ and the stress $\sigma = \Delta P$, then (4) can be rewritten as:

$$S = \frac{\varepsilon}{\sigma(1 - \varepsilon)}. \quad (5)$$

Using (5), sensitivity optimisation is defined as:

$$\max_{\forall e \in E} S(p_t), \quad (6)$$

where $E = \{e_1, \dots, e_n\}$ is the set of elastomers in the database and p_t is the target contact pressure. The sensitivity is implicitly parameterised on E because each elastomer is characterised by values for ε and σ .

Weight optimisation. When robot skin is applied to a large robot surface, its weight becomes non negligible from the payload and control perspectives. In order to increase the overall sensitivity, ceramic fillers are usually added to a base elastomer [10]. However, such fillers increase the compound elastomer's density and, therefore, sensor weight. The toolbox provides the possibility of considering the weight as an optimisation objective:

$$\min_{\forall e \in E} W(p_t), \quad (7)$$

where W is defined as:

$$W = \rho_e \Lambda d_n. \quad (8)$$

In (8), ρ_e is the density of the selected elastomer e in g/cm^3 , Λ is the patch area in cm^2 , and d_n is the elastomer nominal thickness. The latter greatly affects the overall robot skin weight. Given an applied pressure p_t , each elastomer is characterised by a different strain, which leads to a required minimum elastomer-dependent thickness to avoid saturation. The toolbox computes such a minimum thickness on the basis of the selected pressure p_t and it uses this value to compute the

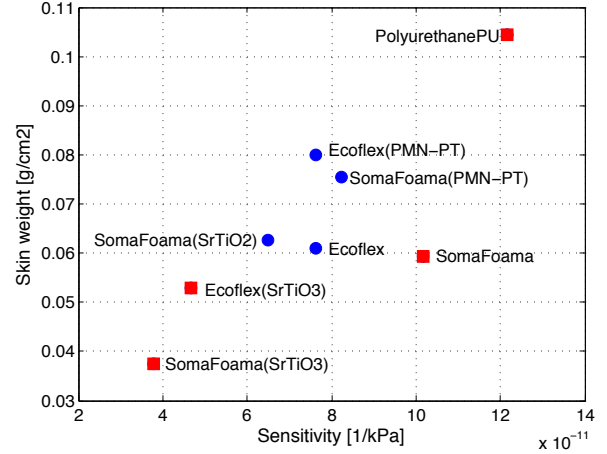


Fig. 7. Pareto front for a pressure of 10 KPa.

weight. As an example, given a desired target contact pressure of 10 KPa to be detected by a single triangular module, the toolbox selects SomaFoama filled with $SrTiO_3$ as the most appropriate material, and computes a minimum thickness of 0.246 mm to obtain the lightest elastomer for the selected pressure.

Multi-objective optimisation. Often, compromise solutions between sensitivity and weight must be found. Currently, the problem is formalised as:

$$\max_{\forall e \in E} [S(p_t), -W(p_t)], \quad (9)$$

where $S(p_t)$ is the sensitivity function defined in (5) and $W(p_t)$ is the weight function in (7).

For these multi-objective optimisation problems, it may be the case that no unique solution exists optimising both objective functions. However, a number of Pareto optimal solutions could actually exist. A solution is called *Pareto optimal* if no objective function can be improved without degrading (at least) another objective values. Formally, $e_1 \in E$ is said to *Pareto dominate* another solution $e_2 \in E$ if:

- $f_i(e_1) \leq f_i(e_2)$ for all indices $i = \{1, 2\}$, and
- $f_j(e_1) < f_j(e_2)$ for at least one index $j = \{1, 2\}$,

where in our case $f_1 = S$ and $f_2 = -W$. A solution $e_1 \in E$ is called Pareto optimal if there is no other solution dominating it. The set of Pareto optimal solutions $f_i(e_1)$ with $i = \{1, 2\}$ is called *Pareto front* or *Pareto boundary*.

Depending on the selected range for the applied pressure, the goal of multi-objective optimisation is to find a representative set of Pareto optimal solutions to allow a robot skin designer to quantify the trade-off of each solution in satisfying the different objectives and in taking a decision about the elastomer to use.

Figure 7 shows sensitivity and weight computed for each elastomer for a target pressure $p_t = 10$ KPa. There are four Pareto optimal solutions highlighted with red squares. It is noteworthy that the *lightest* material, namely SomaFoama filled with $SrTiO_3$, is also the less sensitive, whereas the most

sensitive material, namely Polyurethane, is also the *heaviest*. In this case, the selection is made on the basis of the particular application. For instance, between the two solutions Ecoflex filled with SrTiO_3 and SomaFoama, the latter could be chosen since, in spite of being slightly heavier, is characterised by a higher sensitivity.

IV. EXPERIMENTAL VALIDATION AND DISCUSSION

Results provided by the toolbox have been validated using real experiments as a ground truth. In particular, we wanted to assess the toolbox capabilities in a real-world scenario using data from a robot skin patch integrated on the palm of the iCub robot [3] and used for several months, in order to include in the validation the variability and the effects of ageing as discussed in Section III-A. Three tests are reported: (i) assessment of taxel capacitance variations; (ii) robustness with respect to material characterisation parameters; (iii) spatial response with respect to known contact areas. Furthermore, we replicated the same experiments shown and discussed in [3]. A specific taxel is stimulated using an indenter located at the end-effector of a Cartesian robot provided with a load cell for force sensing. Different cylindrical probes of varying diameters (respectively, 4, 5 and 6 mm) are used. A sequence of peak-increasing pressure distributions are imposed, with a 0.1 mm depth resolution. At each depth, probes are maintained in firm contact position for around 2 sec, and subsequently are moved upward. After 20 sec, the subsequent contact depth is set as the next reference, in order to minimise the effects of material hysteresis on the measurements.

The same experimental conditions have been replicated in the toolbox. The same pressure detected by the load cell in real experiments is applied to an area equivalent to the real one. The structural mechanics component computes the elastomer deformation on the basis of the applied pressure and, according to it, the electrostatics component computes the capacitance values for each interested taxel.

Figure 8 shows a comparison between experimental and simulated data when probes of different size are used. It can be noticed that experimental and simulation results agree until the value of the exerted pressure reaches approximately 20 KPa. When this happens, simulation results deviate from experimental ones as long as the applied pressure increases, reaching an error of 10% of the sensor response in the characterised pressure range for both 4 mm and 5 mm probes and reaching 21.45% and 30% for 4 mm and 5 mm probes, respectively, for the maximum exerted pressure. A greater error outside the characterised range is reasonable since the mechanical characteristics of the elastomer are the result of an interpolation, as discussed above. As anticipated, this difference results from the specific characterisation of the particular elastomer sample: the SomaFoama sample whose characterisation is present in the toolbox database is different from the sample covering the iCub palm, which presents also ageing effects. As an evidence of these aspects, the error is coherent with the standard deviation reported in Figure 5(a).

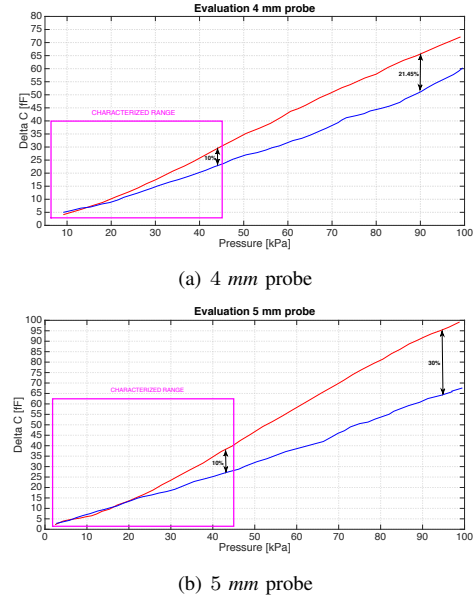


Fig. 8. Comparison between experimental and simulation data for a 4, 5 and 6 mm probe. Blue lines: experimental data; red lines: simulation data.

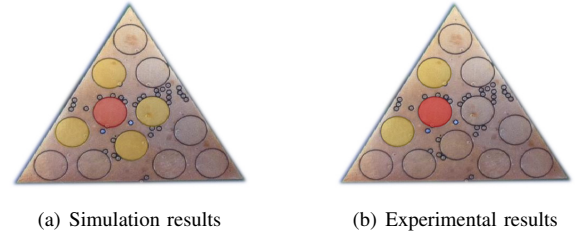


Fig. 9. Comparison between simulation and experimental data related to taxel spatial responses. The red taxel is where the pressure is applied, yellow ones are excited due to elastomer deformation.

Taking into account the considerations above, simulations are a working approximation of experimental results.

Lesson learnt number 1: material characterisation is fundamental to obtain realistic simulations.

Regarding the spatial activation of taxels, a comparison between simulation and experimental results is shown in Figure 9. The Figure refers to the application of a 50 KPa pressure using a 6 mm probe. In simulation, the 4 taxels around the mechanically stressed one are activated, whereas in real experiments only two are. This behaviour can be explained by the fact that the pressure area in the simulation is perfectly centred on the taxel, whereas in the experimental results a little displacement affects the spatial taxel activation.

Lesson learnt number 2: it is hard to make experimental set-ups and simulations consistent.

In order to validate the toolbox contact modelling capabilities, we refer to two scenarios. In the first, an *object manipulation* pressure and a *keyboard* contact area are selected. For a triangular module, the default geometric configuration is used, with a SomaFoama filled with PMN-PT dielectric layer. In the second, a *gentle touch* pressure has been chosen, whereas

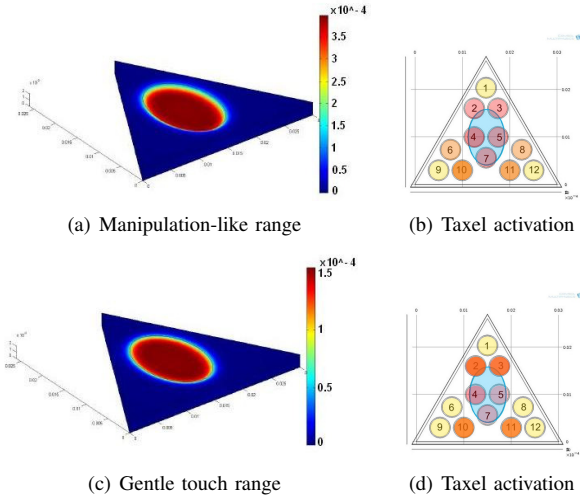


Fig. 10. Two simulated scenarios.

other parameters remain the same. Displacement results are shown in Figure 10(a) and Figure 10(c) as displacement fields, whereas in Figure 10(b) and Figure 10(d) the related tactel activations are shown, with a color gradient from red to yellow, where red represents activated tactels and yellow unaffected ones. In this case, results in simulation are consistent with real-world experiments.

Lesson learnt number 3: considering a specific scenario is fundamental to obtain good design results.

V. CONCLUSION

This paper describes a toolbox for the design and simulation of capacitance-based tactile sensors, and discusses the main limitations associated with the simulation process. The toolbox is composed of two parts: the analysis component allows designers to set parameters and simulate the corresponding sensor behaviour, whereas the optimisation component provides information about the selection of the proper elastomer to use on the basis of user requirements. FEM analyses are employed, which use the deformed mesh principle to obtain a multiphysics simulation. Optimisation processes are based on a database of characterised elastomers, which has been collected in the past few years. Models and simulation results are described, showing that this approach is a viable solution to investigate a number of system-level features otherwise difficult to assess with real experiments, because of the necessity of having different technological samples, in terms of cost and time. The intrinsic limitations associated with the simulation process are exposed as well, which contributes to a fair discussion about the employability of such a simulation framework. The toolbox is available as free software.

ACKNOWLEDGMENT

The research leading to these results has received funding from the European Community's Seventh Framework Programme (FP7/2007-2013) under Grant Agreement no. 231500 (Project ROBOSKIN) and no. 288553 (Project CloPeMa).

REFERENCES

- [1] R. Dahiya, G. Metta, M. Valle, and G. Sandini, "Tactile sensing: from humans to humanoids," *IEEE Transactions on Robotics*, vol. 26, no. 1, pp. 1–20, February 2010.
- [2] A. Billard, A. Bonfiglio, G. Cannata, P. Cosseddu, T. Dahl, K. Dautenhahn, F. Mastrogiovanni, G. Metta, L. Natale, B. Robins, L. Seminara, and M. Valle, "The ROBOSKIN project: challenges and results," in *Romansy 19 - Robot Design, Dynamics and Control*, ser. CISM International Centre for Mechanical Sciences, V. Padois, P. Bidaud, and O. Khatib, Eds. Springer Vienna, 2005, vol. 544, pp. 351–358.
- [3] A. Schmitz, P. Maiolino, M. Maggiali, L. Natale, G. Cannata, and G. Metta, "Methods and technologies for the implementation of large-scale robot tactile sensors," *IEEE Transactions on Robotics*, vol. 27, no. 3, pp. 389–400, June 2011.
- [4] D. Anghinolfi, G. Cannata, F. Mastrogiovanni, C. Nattero, and M. Paolucci, "On the problem of the automated design of large-scale robot skin," *IEEE Transactions on Automation Science and Engineering*, vol. 10, no. 4, October 2013.
- [5] E. Baglini, S. Youssefi, F. Mastrogiovanni, and G. Cannata, "A real-time distributed architecture for large-scale tactile sensing," in *Proceedings of the 2014 IEEE/RSJ International Conference on Intelligent Robots and Systems (IROS 2014)*, Chicago, IL, USA, September 2014.
- [6] S. Denei, F. Mastrogiovanni, and G. Cannata, "Towards the creation of tactile maps for robots and their use in robot contact motion control," *Robotics and Autonomous Systems*, vol. 63, pp. 293–308, January 2015.
- [7] S. Youssefi, S. Denei, F. Mastrogiovanni, and G. Cannata, "A real-time data acquisition and processing framework for large-scale robot skin," *Robotics and Autonomous Systems*, vol. 68, pp. 86–103, June 2015.
- [8] J. A. Rogers, T. Someya, and Y. Huang, "Materials and mechanics for stretchable electronics," *Science*, vol. 327, no. 5973, pp. 1603–1607, 2010.
- [9] K. Johnson, *Contact Mechanics*. Cambridge, UK: Cambridge University Press, 1985.
- [10] P. Maiolino, F. Galantini, F. Mastrogiovanni, G. Gallone, G. Cannata, and F. Carpi, "Soft dielectrics for capacitive sensing in robot skins: performance of different elastomer types," *Sensors and Actuators A*, vol. 226, pp. 37–57, May 2015.
- [11] S. Yahud, S. Dokos, J. Morley, and N. Lovell, "Finite element analysis of a tactile sensor for a robotic hand," in *Proceedings of the 2008 International Conference on Intelligent Sensors, Sensor Networks and Information Processing (ISSNIP'08)*, Brisbane, Australia, December 2010.
- [12] Y. Zhang, "Sensitivity enhancement of a micro-scale biomimetic tactile sensor with epidermal ridges," *Journal of Micromechanics and Micro-engineering*, vol. 20, no. 8, August 2010.
- [13] M. Tiwanaa, A. Shashankb, S. Redmondb, and N. Lovella, "Characterization of a capacitive tactile shear sensor for application in robotic and upper limb prostheses," *Sensors and Actuators A: Physical*, vol. 165, no. 2, pp. 164–172, February 2011.
- [14] R. Ellis and M. Qin, "Finite-element and singular-value analysis of tactile sensors," in *Proceedings of the 1994 IEEE International Conference on Robotics and Automation (ICRA 1994)*, San Diego, CA, USA, May 1994.
- [15] M. Shimojo, "Mechanical filtering effect of elastic cover for tactile sensors," *IEEE Transactions on Robotics and Automation*, vol. 13, no. 1, pp. 128–132, February 1997.
- [16] L. Le, M. Zoppi, M. Jilich, H. Bo, D. Zlatanov, and R. Molino, "Application of a biphasic actuator in the design of the CloPeMa robot gripper," *Journal of Mechanisms and Robotics*, vol. 7, no. 1, Feb 2015.
- [17] I. Ward and J. Sweneey, *An Introduction To Mechanical Properties Of Solid Polymers*. Wiley and Sons Ltd., 2004.
- [18] S. Mannsfeld, B. Tee, R. Stoltenberg, C. Chen, S. Barman, B. Muir, A. Sokolov, C. Reese, and Z. Bao, "Highly sensitive flexible pressure sensors with microstructured rubber dielectric layers," *Nature Materials*, vol. 9, pp. 859–864, September 2010.
- [19] H. Alirezai, A. Nagakubo, and Y. Kuniyoshi, "A highly stretchable tactile distribution sensor for smooth surfaced humanoids," in *Proceedings of the 2007 IEEE-RAS International Conference on Humanoid Robots (HUMANOIDS 2007)*, Pittsburgh, PA, USA, December 2007.
- [20] Y. Fujimori, Y. Ohmura, T. Harada, and Y. Kuniyoshi, "Wearable motion capture suit with full-body tactile sensors," in *Proceedings of the 2009 International Conference on Robotics and Automation (ICRA 2009)*, Kobe, Japan, May 2009.